

Stop and sbottom search using dileptonic M_{T2} variable and boosted top technique at the LHC

Amit Chakraborty^a, Dilip Kumar Ghosh^a, Diptimoy Ghosh^b, Dipan Sengupta^c

^a Department of Theoretical Physics, Indian Association for the Cultivation of Science,
2A & 2B, Raja S.C. Mullick Road, Jadavpur, Kolkata 700 032, India

^b INFN, Sezione di Roma,
Piazzale A. Moro 2, I-00185 Roma, Italy

^c Department of High Energy Physics, Tata Institute of Fundamental Research,
1, Homi Bhabha Road, Mumbai-400 005, India

Abstract

The ATLAS and CMS experiments at the CERN LHC have collected about 25 fb^{-1} of data each at the end of their 8 TeV run, and ruled out a huge swath of parameter space in the context of Minimally Supersymmetric Standard Model (MSSM). Limits on masses of the gluino (\tilde{g}) and the squarks of the first two generations (\tilde{q}) have been pushed to above 1 TeV. Light third generation squarks namely stop and sbottom of sub-TeV masses, on the other hand, are still allowed by their direct search limits. Interestingly, the discovery of a Standard Model (SM) higgs boson like particle with a mass of $\sim 125 \text{ GeV}$ favours a light third generation which is also motivated by naturalness arguments. Decays of stop and sbottom quarks can in general produce a number of distinct final states which necessitate different search strategies in the collider experiments. In this paper we, on the other hand, propose a general search strategy to look for third generation squarks in the final state which contains a top quark in the sample along with two additional hard leptons and substantial missing transverse momentum. We illustrate that a search strategy using the dileptonic M_{T2} , the effective mass m_{eff} and jet substructure to reconstruct the hadronic top quark can be very effective to reduce the SM backgrounds. With the proposed search strategy, we estimate that the third generation squarks with masses up to about 900 GeV can be probed at the 14 TeV LHC with 100 fb^{-1} luminosity. We also interpret our results in two simplified scenarios where we consider the stop (sbottom) pair production followed by their subsequent decay to a top quark and the second lightest neutralino (lightest chargino). In this case also we find that stop (sbottom) mass up to 1 TeV (0.9 TeV) can be discovered at the 14 TeV LHC with 100 fb^{-1} integrated luminosity.

PACS numbers: 11.30pb, 14.80Ly, 14.80Nb

Contents

1	Introduction and motivation	2
2	Choice of model parameters, benchmarks and branching ratios	4
3	Details of collider simulation and results	5
4	Interpretation in simplified scenarios	11
5	Summary and Conclusion	12
6	Acknowledgements	12

1 Introduction and motivation

As the LHC suspends its operation for the upgrade to 14 TeV after having collected about 25 fb^{-1} of data by each of the ATLAS [1] and CMS [2] experiments at the centre of mass energy of 8 TeV, we look back and marvel at the amazing performance of the machine and the breakneck pace at which the ATLAS and CMS collaborations have been analyzing the data. The feather in the cap of the 8 TeV run has been the most anticipated result in particle physics in the last two decades; the discovery of a boson of mass about 125 GeV which resembles the standard model(SM) higgs boson in its behavior [3, 4].

The discovery of a 125 GeV higgs like boson has fueled speculations of physics beyond the SM from various considerations like vacuum stability, fine tuning of the higgs potential and so on. The impact of this discovery on new physics scenarios has been studied extensively in the recent past. Its implications on Supersymmetry(SUSY) have been discussed in a wide range of papers [5–33]. Along with this there have been sustained efforts in the particle physics community to probe SUSY signatures in the light of the recent higgs data [34–45]. While after the first two years of data taking the gluinos and first two generation of squarks do not seem to be in the sub-TeV scale, the discovery of the higgs like boson has spurred a renewed interest in a region of SUSY parameter space termed as “natural Supersymmetry” [12, 20, 46–49]. This idea stems from the fact that the most relevant superparticles responsible for cancellation of the quadratic divergence in the higgs mass are the third generation squarks. Therefore, even if squarks of the first two generations and the gluinos are heavy, a comparatively lighter third generation can cure the fine-tuning problem in the SM. While a 125 GeV higgs would, in general, necessarily mean a large stop tri-linear coupling A_t , introducing some adjustment of parameters in the theory, a light third generation scenario nevertheless has an extremely attractive prospect for both the theorists and the experimentalists. This has brought about a paradigm shift in the way SUSY searches have been conducted at the LHC.

At the LHC the SUSY searches have been performed quite extensively both in the framework of constrained minimally supersymmetric standard model (cMSSM) which assumes specific relations among the soft supersymmetry breaking couplings at a very high energy scale and in other models which relax these simplifying assumptions to various degrees. There have been quite a few phenomenological analysis to investigate cMSSM signatures at the LHC using different techniques to suppress SM background [21, 37, 38]. The limit on the gluino mass obtained by ATLAS and CMS collaborations in the cMSSM context currently stands at about 1.5 TeV for $m_{\tilde{g}} \simeq m_{\tilde{q}}$ and about 1.2 TeV for $m_{\tilde{g}} \ll m_{\tilde{q}}$ [50, 51]. More recently, however, other models specially R-parity violating SUSY models and gauge mediated supersymmetry breaking scenarios have also been studied by both ATLAS [52, 53] and CMS [54, 55] collaborations.

While cMSSM searches have provided a guideline to the way collider strategies are devised at the LHC, the negative results in all the searches have triggered a more pragmatic approach to SUSY searches at the LHC. This together with the discovery of a SM higgs like boson has lead us to look beyond cMSSM, in particular at considering simplified models motivated by naturalness arguments and hence, light third generation particles in a general MSSM framework with no specific relations among the soft supersymmetry breaking parameters. This has motivated an avalanche of phenomenological studies in light stops and/or light sbottom scenarios [40, 46, 47, 56–72]. In terms of collider searches most phenomenological studies have been conducted for predominantly right handed stop and sbottom quarks in the decay channels $\tilde{t} \rightarrow t\tilde{\chi}_1^0$

and $\tilde{b}_1 \rightarrow b\tilde{\chi}_1^0$ [67, 73–76]. The general observation has been that the efficiency depends strongly on the $\tilde{t}_1(\tilde{b}_1) - \tilde{\chi}_1^0$ mass difference which, if large, leads to a hard jets and a large missing transverse energy (\cancel{E}_T) crucial in suppressing the large background arising from the production of top quarks in the SM, while for smaller mass difference scenarios it has been suggested to look for stop pair production in association with one hard QCD jet prompting monojet + \cancel{E}_T final state [57, 58]. Some analyses have tried to overcome this problem by performing a shape analysis of the distributions of \cancel{E}_T and \cancel{E}_T -related observables [70]. It has also been suggested that in the large $\tilde{t}_1 - \tilde{\chi}_1^0$ mass difference scenario, the use of top-tagging by jet substructure methods can also be very helpful in achieving a reasonable sensitivity both from direct stop production and in stops from gluino cascade decays [68, 77–80].

Recently several phenomenological studies have been performed to investigate the signature of strongly interacting third generation SUSY particles in various channels at the 14 TeV run of the LHC. A monojet with large \cancel{E}_T signal has been proposed to look for the light stop, where $\tilde{t}_1 \rightarrow c\tilde{\chi}_1^0$ via one loop processes. Using this signal topology, it has been found with 100 fb^{-1} luminosity a light stop mass up to 250 GeV can be probed [58]. Similarly the prospect of a spin zero top partner decaying to top quark and neutral particles was also studied in [63] and the expected discovery limit for light stop mass is close to 675 GeV with 100 fb^{-1} luminosity. The gluino-stop-neutralino model has been also studied in [68] with two top tagged jets and missing energy. The resultant gluino discovery limit is expected to be 1.7 TeV with 33 fb^{-1} luminosity. As far as the sbottom searches are concerned, it has been shown that in the sbottom-co-annihilation scenario $\tilde{b}_1 \rightarrow b\tilde{\chi}_1^0$ the light sbottom mass up to 570 GeV can be observed once again with 100 fb^{-1} data [73].

As far as the experimental efforts to look for the signal of stop and sbottom at the LHC are concerned, both the ATLAS and the CMS Collaborations have searched for light stops in simplified models and placed limits assuming specific mass relations among gluino, stop and the lightest neutralino. The CMS collaboration analyzed about 10.5 fb^{-1} of data set at 8 TeV center of mass energy in the same sign di-lepton + b-tagged jets final state and placed limits in various simplified model scenarios [81]. This study ruled out up to 1 TeV gluino mass in a model where the gluino decays via an off-shell stop, $\tilde{g} \rightarrow t\tilde{t}_1^* \rightarrow t\tilde{t}_1\tilde{\chi}_1^0$, for the lightest neutralino mass up to 600 GeV. The same study also excluded gluino mass up to 1 TeV, where gluino decays via on shell top and stop to the same final state as above for $m_{\tilde{t}_1} \simeq 800 \text{ GeV}$ and $m_{\tilde{\chi}_1^0} = 50 \text{ GeV}$. They also examined models where the gluino cascades via on-shell sbottoms to charginos and finally to di-leptons ($\tilde{g} \rightarrow \tilde{b}b \rightarrow t\tilde{\chi}_1^\pm b$). This study ruled out gluino masses in the range 300 GeV – 1 TeV for sbottom masses in the same range assuming $\tilde{\chi}_1^0$ and $\tilde{\chi}_1^\pm$ masses to be 50 GeV and 150 GeV respectively. Finally, from the direct sbottom production process sbottom masses in the window 270 – 450 GeV for $\tilde{\chi}_1^\pm$ masses in the range 100 – 200 GeV with a $\tilde{\chi}_1^0$ mass of 50 GeV are excluded. The ATLAS collaboration recently searched for light stops in the channel $\tilde{t}_1 \rightarrow b\tilde{\chi}_1^\pm \rightarrow b\tilde{\chi}_1^0 f f'$ assuming $\Delta m \equiv m_{\tilde{\chi}_1^\pm} - m_{\tilde{\chi}_1^0}$ to be 5 GeV and 20 GeV. For $\Delta m = 5 \text{ GeV}$ they ruled out stop masses of about 600 GeV in a corridor of lightest neutralino mass [82]. ATLAS also studied light stops in the decay mode $\tilde{t}_1 \rightarrow \tilde{b}\tilde{\chi}_1^\pm$ and $\tilde{t}_1 \rightarrow t\tilde{\chi}_1^0$ with 20.7 fb^{-1} of data in the final state with a single lepton in association with jets(including one b-tagged jet) and \cancel{p}_T [83] using the kinematic variable M_{T2} . Assuming 100% branching ratio for $\tilde{t}_1 \rightarrow t\tilde{\chi}_1^0$ this study ruled out light stop masses between 200 and 610 GeV assuming massless LSP, while a stop of up to 500 GeV was ruled out for LSP masses up to 250 GeV. In the $\tilde{t}_1 \rightarrow \tilde{b}\tilde{\chi}_1^\pm$ channel, this study ruled out stop masses up to 410 GeV assuming a chargino mass of 150 GeV. In the no lepton + jets+ \cancel{p}_T final state ATLAS looked for stops and sbottoms in the channels $\tilde{t}_1 \rightarrow b\tilde{\chi}_1^\pm$, and $\tilde{b}_1 \rightarrow b\tilde{\chi}_1^0$ with the use of the contranverse mass variable m_{CT} [84]. This study ruled out sbottom masses up to 620 GeV for a lightest neutralino mass below 150 GeV. The same study also ruled out stop masses up to 580 (440) GeV for $\Delta m = m_{\tilde{\chi}_1^\pm} - m_{\tilde{\chi}_1^0} = 5(20) \text{ GeV}$ assuming a LSP mass of 100 GeV. Along with these there have been studies in the di-lepton channel for stops decaying via the above mode [85], while stops in other model scenarios like gauge mediated supersymmetry breaking scenario(GMSB) has also been considered [86]. Stop searches by ATLAS at 7 TeV LHC in all the above mentioned channels also provided limits in this respect [87–89]. Similar studies have also been performed by the CMS collaborations and the most updated results can be found in Ref. [90, 91].

It is imperative for some of these search strategies to be extended and made more efficient to cover more ground in the quest for strongly interacting third generation SUSY. Among the various final states that can be analyzed, it is also worthwhile to consider a general strategy for stop and sbottom quarks such that the same final state is common to both the stop and sbottom pair production. Although, light stops and/or light sbottoms around or below the TeV scale is well motivated, production cross sections for individual stop

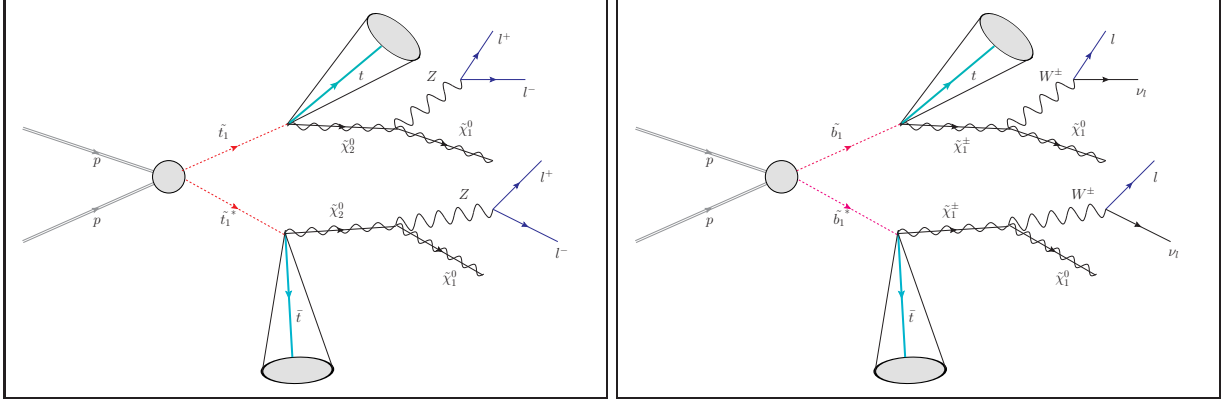


Figure 1: Sample Feynman diagrams for stop and sbottom pair productions and their subsequent decays to a final state containing a top quark, two additional leptons and missing transverse momentum.

pair and sbottom pair process are rather small even at 14 TeV LHC and thus, the option of an inclusive stop and sbottom search is lucrative, as was the case for early inclusive cMSSM searches at the LHC for squarks and the gluino. This motivates us to consider the final state containing a hadronic top quark, two additional hard leptons and missing transverse momentum which can originate from the decays of both the stop and sbottom pairs. Some of the decay chains which can give rise to such final state are shown below,

$$\begin{aligned}
 pp &\rightarrow \tilde{t}_1 \tilde{t}_1^* \rightarrow t \bar{t} \tilde{\chi}_2^0 \tilde{\chi}_2^0 \rightarrow t \bar{t} + 2Z + 2\tilde{\chi}_1^0 \rightarrow t/\bar{t} + \ell\ell + \cancel{p}_T + X \\
 pp &\rightarrow \tilde{t}_1 \tilde{t}_1^* \rightarrow t \bar{b} \tilde{\chi}_2^0 \tilde{\chi}_1^- \rightarrow t \bar{b} + W^- Z + 2\tilde{\chi}_1^0 \rightarrow t + \ell\ell + \cancel{p}_T + X \\
 pp &\rightarrow \tilde{t}_1 \tilde{t}_1^* \rightarrow t \bar{b} \tilde{\chi}_2^0 \tilde{\chi}_1^- \rightarrow t \bar{b} + W^- h + 2\tilde{\chi}_1^0 \rightarrow t + \ell\ell + \cancel{p}_T + X \\
 pp &\rightarrow \tilde{b}_1 \tilde{b}_1^* \rightarrow t \bar{t} \tilde{\chi}_1^+ \tilde{\chi}_1^- \rightarrow t \bar{t} + W^+ W^- + 2\tilde{\chi}_1^0 \rightarrow t/\bar{t} + \ell\ell + \cancel{p}_T + X \\
 pp &\rightarrow \tilde{b}_1 \tilde{b}_1^* \rightarrow t \bar{b} \tilde{\chi}_1^- \tilde{\chi}_2^0 \rightarrow t \bar{b} + W^- Z + 2\tilde{\chi}_1^0 \rightarrow t + \ell\ell + \cancel{p}_T + X.
 \end{aligned}$$

where, $\ell = e$ and μ .

In Fig. 1 we also show two example Feynman diagrams of the processes of our interest. Note that, if the stops and sbottoms are moderately heavy with a large mass gap $\tilde{b}_1 - \tilde{\chi}_1^\pm$ and $\tilde{t}_1 - \tilde{\chi}_2^0$, the produced top quark can be sufficiently energetic so that the jet substructure techniques can be very useful to reconstruct them in the hadronic channel. Along with this, two additional hard leptons with moderately large missing transverse energy can lead to a clean signal. In addition to reconstructing a boosted top quark, a hard cut on M_{T2} constructed out of the momenta of the two hard leptons and the missing transverse energy helps us to combat the background in an efficient way.

We organize our paper as follows. In section 2 we discuss the choice of our model parameters. A few benchmark points are also selected for the illustration of our collider strategy. Section 3 describes the details of our event selection cuts. The signal, backgrounds and statistical significance are also shown. The interpretation of our results in two simplified models is presented in section 4 and finally, we summarize our observations and conclude in section 5.

2 Choice of model parameters, benchmarks and branching ratios

In models like cMSSM where all the scalar soft masses are set to a common value at a high scale, the lightest stop squark, because of the large Renormalization Group(RG) effect, becomes predominantly right handed. A bino-like lightest neutralino also often emerges from the minimal supergravity boundary conditions. Because of this, light third generation searches so far have been mostly carried out in the scenario where the dominant decay modes for the top and bottom squarks are $\tilde{t}_1 \rightarrow t\tilde{\chi}_1^0$ and $\tilde{b}_1 \rightarrow b\tilde{\chi}_1^0$ (Provided $\tilde{t}_1 - \tilde{\chi}_1^0$ mass gap is sufficient for this decay to be kinematically allowed).

However, decays of top and bottom squarks to the heavier neutralinos and charginos are quite motivated in the context of natural SUSY spectrum and have gained considerable attention recently [92, 93]. The branching ratios to these channels can also be quite high in many scenarios [92, 93]. In the context of

the phenomenological MSSM (pMSSM) this can easily be achieved by having the lighter stop and sbottom predominantly left handed. In this case the decays of stop and sbottom will be dominated by $\tilde{t}_1 \rightarrow t\tilde{\chi}_2^0$, $\tilde{t}_1 \rightarrow b\tilde{\chi}_1^+$ and $\tilde{b}_1 \rightarrow b\tilde{\chi}_2^0$, $\tilde{b}_1 \rightarrow t\tilde{\chi}_1^-$ respectively. With the increasing masses of the top and bottom squarks the modes $\tilde{t}_1 \rightarrow t\tilde{\chi}_{3,4}^0$, $\tilde{t}_1 \rightarrow b\tilde{\chi}_2^+$ and $\tilde{b}_1 \rightarrow b\tilde{\chi}_{3,4}^0$, $\tilde{b}_1 \rightarrow t\tilde{\chi}_2^-$ also open up. While these latter decay modes allow a plethora of final states which can be studied individually, all of them also contribute to the final state of our interest. Thus, our analysis also captures some of the events arising from these decay chains.

In order to perform a detailed analysis of signal and background which we present in the next section, we now choose a few model benchmark points. Note that both the ATLAS and CMS collaborations have searched for electroweak gauginos in the channel $pp \rightarrow \tilde{\chi}_1^\pm \tilde{\chi}_2^0 \rightarrow W\tilde{\chi}_1^0 Z\tilde{\chi}_1^0$ which have ruled out a range $\tilde{\chi}_1^\pm = \tilde{\chi}_2^0$ masses as a function of the LSP mass [94–96]. Here, we would like to emphasize that in their analysis the second neutralino is always assumed to decay exclusively to the LSP and the Z boson and hence the limits obtained there will not apply directly for the case where the second neutralino has non zero branching ratio to the higgs boson also. In order to be more general, we will consider two different scenarios: in one case the dominant decay mode of the second lightest neutralino is via the Z boson (benchmarks P2, P3, P6) and in the other case the second lightest neutralino decays dominantly via the higgs (benchmarks P1, P4, P5). In order to do that, the gluino mass parameter M_3 is set to 1.5 TeV as it is irrelevant for the parameter space of our interest and the values of M_1 and M_2 are varied, hence providing various values of $\tilde{\chi}_i^0$ and $\tilde{\chi}_i^\pm$ (see Table 1) to obtain various decay scenarios so as to make our search strategy fairly generic. The higgsino mass parameter μ is taken to be 300 GeV and $\tan\beta$, the ratio of the vacuum expectation values of the two higgs doublets, is fixed at the value of 10.

The right handed third generation squark mass parameters $m_{\tilde{t}_R}$ and $m_{\tilde{b}_R}$ are set to a high value of 2 TeV in order to keep the lightest stop and sbottom mostly left handed facilitating the dominance of the decay modes of our interest. All the tri-linear couplings, with the exception of A_t , is set to zero. A_t is taken to have a large negative value of -2800 GeV just to make sure that the lightest higgs mass is in the range 123 – 128 GeV. These tri-linear couplings, however, have very little bearing on our final results. The masses of the first two generations of squarks and all the three generations of sleptons are set to 5 TeV as they are irrelevant for our study.

To generate the physical masses of the sparticles we have used the software package SuSpect [97]. The decay branching ratios are then calculated using SUSYHIT [98] which also includes SuSpect inside it. In Table 1 we present the masses of top and bottom squarks along with the neutralino, chargino states and the relevant branching ratios for the six benchmark points which we choose for our signal and background analysis in the next section. The light stop and sbottom masses are obtained by varying the left handed third generation squark mass parameter $m_{\tilde{Q}_3}$ as shown in the first column of Table 1. As we have already mentioned earlier, in order to demonstrate that our search strategy is democratic we choose benchmark points such that $\tilde{\chi}_2^0$ decays via both the Z boson and/or the Higgs boson. Along with these we also provide the cross section for the $\tilde{\chi}_1^\pm \tilde{\chi}_2^0$ pair production at 8 TeV such that a rough estimate of the experimental bounds can be checked.

It is worth mentioning that the cross-section for stop or sbottom pair production decreases rapidly with their increasing masses. For example, the next to leading order cross-section for a 500 GeV stop or sbottom pair production stands at around 680 fb (calculated using PROSPINO [99] with the default choices of the scale and parton distribution functions) and goes down to as low as 10 fb for masses of 1 TeV even with the proton proton centre of mass energy of 14 TeV. Hence, to maximize the possibility to see a signal it is important to have most of the branching ratios contribute to the signal. As we mentioned in the previous section, this was precisely our motivation to consider a final state which is common to many of the decay chains of top and bottom squarks.

3 Details of collider simulation and results

In this section we describe the details of our simulation procedure as well as the kinematic selection cuts for our signal and the backgrounds. But before we do that we would like to remind the readers about the final state we are interested in and also discuss the potential backgrounds for our signal. As we have already mentioned earlier, we are interested in a general search strategy for the third generation squarks and hence we consider the final state consisting of at least a top quark, at least two additional leptons and

	P1	P2	P3	P4	P5	P6
$m_{\tilde{Q}_3}$	500	500	700	700	900	900
$m_{\tilde{t}_1}$	501.7	501.7	714.2	714.2	918.1	918.1
$m_{\tilde{b}_1}$	525.4	525.4	748.4	748.4	918.1	918.1
$m_{\tilde{\chi}_1^0}$	48.5	97.9	146.3	97.8	149.0	198.3
$m_{\tilde{\chi}_2^0}$	193.3	193.9	245.9	244.3	297.9	298.6
$m_{\tilde{\chi}_3^0}$	309.3	309.0	309.2	309.4	408.1	408.0
$m_{\tilde{\chi}_4^0}$	338.5	339.2	364.5	363.9	440.5	441.2
$m_{\tilde{\chi}_1^\pm}$	192.8	192.8	242.7	242.7	297.0	297.0
$m_{\tilde{\chi}_2^\pm}$	338.9	338.9	363.5	363.5	439.8	439.8
$\text{BR}(\tilde{b}_1 \rightarrow b \tilde{\chi}_{2,3,4}^0)(\%)$	34.6	34.5	19.3	19.4	19.4	19.4
$\text{BR}(\tilde{b}_1 \rightarrow t \tilde{\chi}_{1,2}^\pm)(\%)$	65.4	65.5	80.7	80.6	80.6	80.6
$\text{BR}(\tilde{t}_1 \rightarrow t \tilde{\chi}_{2,3,4}^0)(\%)$	34.9	35.2	62.5	62.4	62.5	62.5
$\text{BR}(\tilde{t}_1 \rightarrow b \tilde{\chi}_{1,2}^\pm)(\%)$	65.1	64.8	37.5	37.6	37.5	37.5
$\text{BR}(\tilde{\chi}_2^0 \rightarrow \tilde{\chi}_1^0 Z)(\%)$	33.9	100.0	100.0	22.1	12.8	100.0
$\text{BR}(\tilde{\chi}_2^0 \rightarrow \tilde{\chi}_1^0 h)(\%)$	66.1	0.0	0.0	77.9	87.2	0.0
$\sigma(\text{pp} \rightarrow \tilde{\chi}_2^0 \tilde{\chi}_1^\pm)_{8 \text{ TeV}} \text{ (pb)}$	0.671	0.662	0.190	0.196	0.111	0.110

Table 1: Masses of stop, sbottom, neutralinos and charginos and the relevant branching fractions for the six benchmark points. All the other parameters are set to their fixed values as described in the text. In the rows 10-13 the branching fractions to the charginos and neutralinos have been summed over. In the final row, we give the pair production cross-section of lightest chargino and the second lightest neutralino for the 8 TeV LHC. All the masses are in GeV.

some missing transverse momentum. There are several Standard Model processes which can give rise to such final state and thus contribute to the background for our signal. The most important of these backgrounds are $t\bar{t} + n$ jets, $t\bar{t}Z$, $t\bar{t}W$ and $t\bar{b}W$. There are also other backgrounds like $t\bar{t}t\bar{t}$ and $t\bar{t}WW$ but they are expected to be insignificant because of their very low cross-section. In order to check that this is indeed true we also include them in our background estimation. We also check that the tW and tZ events, in spite of their comparatively larger cross-sections [100, 101], do not contribute to the background. Note that, some of the backgrounds mentioned above, at the parton level, do not seem to contribute to the final state of our interest. For example, in $t\bar{t} + n$ jets events once one top is tagged hadronically, there is no possibility of two additional leptons in the final state. However, once parton showering and hadronization is included, an additional lepton can be produced, for example, from a semileptonic B meson decay and thus this process can contribute to our final state.

We are now in a position to discuss the details of our event selection procedure. The reconstruction of final state objects like jets, leptons etc. along with the other selection criteria are described below.

- C1 : At first, we demand at least two isolated leptons (electron and muon) with the transverse momentum $p_T^\ell \geq 25$ GeV and the pseudo-rapidity $|\eta| \leq 3$. Isolation of leptons is ensured by demanding the total transverse energy p_T^{AC} to be less than 20% of p_T^ℓ . Here p_T^{AC} is defined as the scalar sum of transverse momenta of all the hard jets (j) which are close to the lepton satisfying $\Delta R(\ell, j) \leq 0.2$. The jets are formed using the anti- k_T algorithm with the value of $R=0.5$. Out of these jets only the hard jets which satisfy a transverse momentum cut $p_T^j \geq 50$ GeV as well as the the pseudo-rapidity $|\eta| \leq 3$ are selected. The lepton identification at the LHC being extremely efficient and due to the

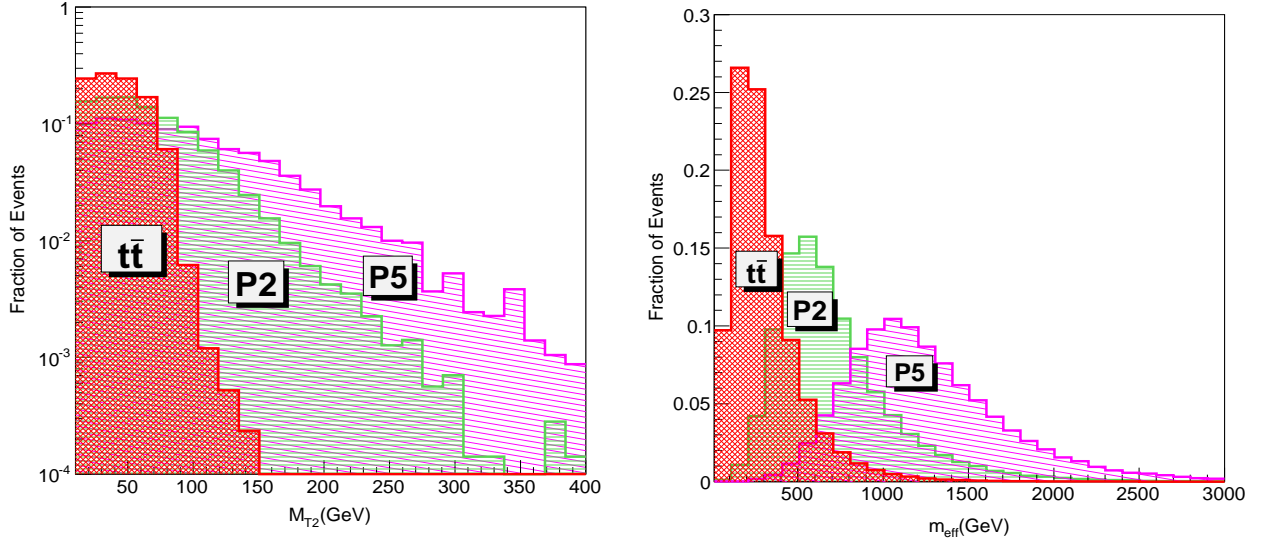


Figure 2: The M_{T2} (left panel) and m_{eff} (right panel) distribution for PYTHIA generated $t\bar{t}$ events (marked as $t\bar{t}$) and two benchmark points (denoted by **P2** and **P5**) with more than 50 fb^{-1} event sample.

clean environment, this can be used as an efficient trigger of our events. Our choice of the final state with two hard and isolated leptons also kills a large part of the SM background.

- C2 : As a second step, we consider the variable M_{T2} [102, 103] which is defined as

$$M_{T2}(\vec{p}_T^{\ell 1}, \vec{p}_T^{\ell 2}, \vec{p}_T^{\text{miss}}) = \min_{\vec{p}_T = \vec{p}_T^1 + \vec{p}_T^2} \left[\max\{M_T(\vec{p}_T^{\ell 1}, \vec{p}_T^1), M_T(\vec{p}_T^{\ell 2}, \vec{p}_T^2)\} \right], \quad (1)$$

where $\ell 1$ and $\ell 2$ are the two hard leptons selected in the previous step, \vec{p}_T^{miss} is the total missing transverse momentum vector of the event and $M_T(\vec{v}_1, \vec{v}_2)$ is the transverse mass of the (\vec{v}_1, \vec{v}_2) system which is defined as

$$M_T(\vec{v}_1, \vec{v}_2) = \sqrt{2|\vec{v}_1||\vec{v}_2|(1 - \cos \phi)},$$

ϕ being the (azimuthal) angle between \vec{v}_1 and \vec{v}_2 . In the definition of Eq.1, \vec{p}_T^1 and \vec{p}_T^2 are a hypothetical split of the total observed missing transverse momentum into two parts. Here we have assumed the masses of the unobserved particles to vanish [104]. As for $t\bar{t}$ events with both the top quarks decaying semi-leptonically the M_{T2} distribution is bounded above by the W boson mass, a hard cut on M_{T2} can help reduce the $t\bar{t}$ background by a significant amount. This can be seen in the left panel of Fig.2 where the M_{T2} distribution for $t\bar{t}$ events as well as two signal points are shown. In our analysis we impose $M_{T2} > 125 \text{ GeV}$ on the events.

- C3 : We now define an effective mass of the system $m_{\text{eff}} = \sum p_T^j + \sum p_T^\ell$, where the first sum runs over all the hard jets and the second sum is over all the hard and isolated leptons present in an event. As m_{eff} is strongly correlated with $2m_{\tau_1}$ or $2m_{\tilde{\nu}_1}$, the signal is expected to occupy the large m_{eff} region of the phase space while the backgrounds should have lower values of m_{eff} . This can be seen in the right panel of Fig.2 where the m_{eff} distribution for $t\bar{t}$ and two signal points are shown. In our analysis, we find a lower cut of $m_{\text{eff}} > 800 \text{ GeV}$ very useful to keep the backgrounds under control while keeping a significant number of signal events.
- C4: As our signal final state consists of a number of stable neutralinos and neutrinos, a moderately hard missing transverse momentum cut $p_T^{\text{miss}} > 150 \text{ GeV}$ is used to further reduce the backgrounds. This step helps to decrease, in particular, the $t\bar{t}$ background to a good extent.

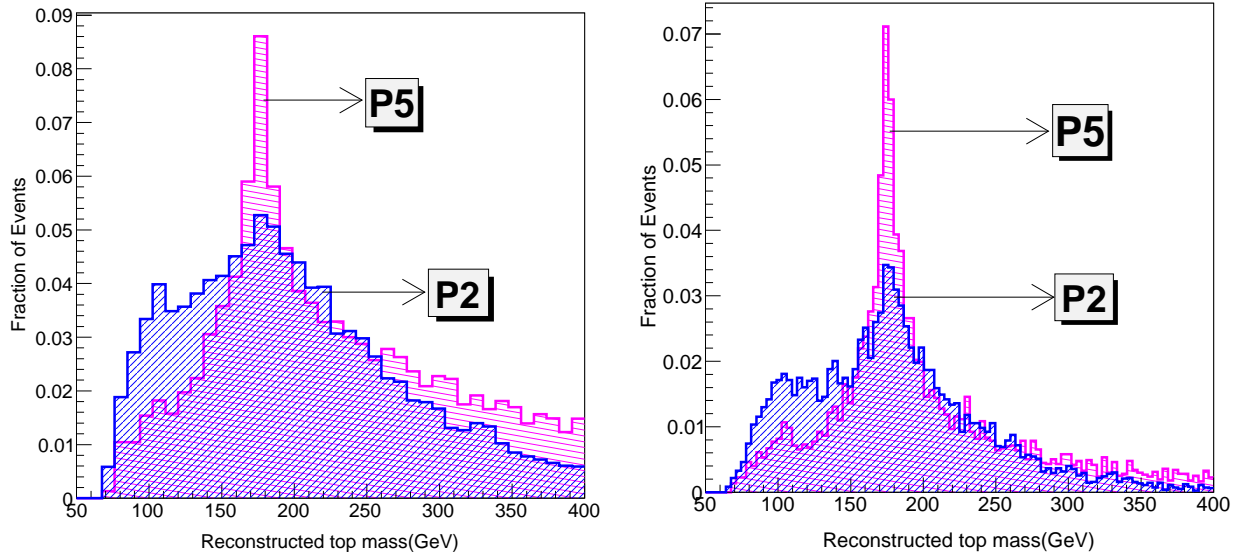
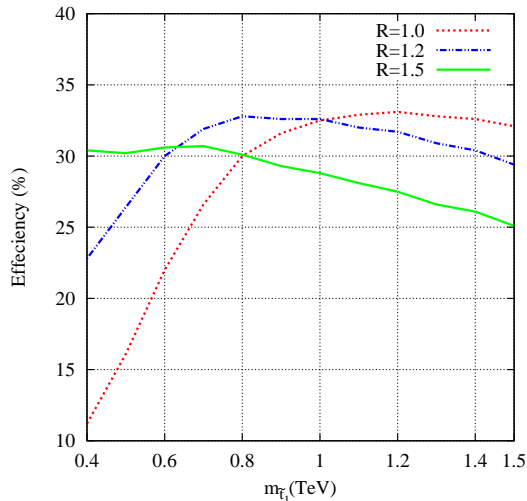


Figure 3: The invariant mass distribution of the reconstructed top quark using the jet substructure algorithm without (left panel) and with (right panel) b-tag (assuming 60% b-tagging efficiency) for two benchmark points with more than 50 fb^{-1} event sample.

- C5 : Finally, we demand at least one top quark in the sample by reconstructing its invariant mass using the jet substructure technique. For this purpose we use the Johns Hopkins top tagger [105], using Cambridge Aachen (C/A) algorithm [106] with the choice of the parameters $R = 1.5$, $\delta_p = 0.10$ and $\delta_r = 0.19$. While reconstructing W mass in the intermediate step of the algorithm we consider the mass window (60-100) GeV and demand that the W helicity angle θ_h satisfies $\cos\theta_h < 0.7$. We demand the final reconstructed top mass to fall in the window (135-215) GeV. We do not impose a b-tag criteria on our reconstructed top quark. The left panel of Fig.3 shows the reconstructed top mass for two of our benchmark points. As the produced top quark is more energetic for heavier stop/sbottom quarks, the jet substructure technique for the top mass reconstruction works better for the benchmark-4. Although we have not used a b-tag criteria in our analysis, in the right panel of Fig.3 we show the improvement of the mass reconstruction if a b-tag is demanded. In Fig.4 we also present the top reconstruction efficiency in the process $pp \rightarrow \tilde{t}_1 \tilde{t}_1^*$, $\tilde{t}_1 \rightarrow t \tilde{\chi}_2^0$ as a function of stop mass for three different values of R assuming the $\tilde{\chi}_2^0$ mass to be 150 GeV. As expected, for $R=1.0$ and $R=1.2$, the efficiency initially increases with the increase in the stop mass, reaches a maximum and then starts decreasing for even larger values of the stop mass. We demand that our choice of R should be optimal for a large region of parameter space. From this figure it is clear that the choice of $R=1.5$ is adequate for our choice of stop mass range. The deviation in the efficiency for other two choices of the parameter R is not more than few percent for our benchmark points.

We use Pythia6.4.24 [107] for generating the signal events. For the backgrounds, we use Madgraph5 [108] to generate parton level events and subsequently use the Madgraph-Pythia6 interface (including matching of the matrix element hard partons and shower generated jets, following the MLM prescription [109]) to perform the showering and implement our event selection cuts. We use the Fastjet3 package [106, 110] for the reconstruction of jets and the implementation of the jet substructure analysis for reconstructing the top quark.

We present our results in Table 2 and 3 where the number of signal and background events surviving after each selection cut are shown respectively. In Table 2 and 3 the first three columns show the processes studied, the raw production cross-section and the number of events generated for each process respectively. For the signal points the raw cross-section corresponds to the next-to-leading-order value calculated using

Figure 4: The top reconstruction efficiency as a function of stop mass for three choices of the parameter R .

Signal	Production Cross-section (fb)	Simulated events (in units of 10^4)	No. of events after the cut					Final Cross-section (in units of 10^{-2} fb)
			C1	C2	C3	C4	C5	
P1	1130	10	10573	821	339	267	55	62.2
P2	1130	10	11091	657	248	205	55	62.2
P3	135	5	8043	1132	712	645	153	41.3
P4	135	5	7713	1207	749	663	153	41.3
P5	27	5	8623	1720	1414	1322	295	15.9
P6	27	5	8543	1679	1343	1281	322	17.4

Table 2: Event summary for the signal after individual cuts as described in the text. In the last column we show the final cross-section after all the event selection cuts have been applied.

Prospino [99] with default choices for the scale and the parton density function. For the background processes we use either the NLO cross-sections if they are available in the literature or the cross-section as given by Madgraph5. For both the signal as well as the backgrounds the total number of events simulated is of the same order or more than the number expected in the 14 TeV LHC with 50fb^{-1} luminosity. In the column 4-8 we show the number of events after each selection cut and the final column shows the cross-section after all the cuts have been imposed. A closer look on the numbers in Table 2 shows how with the increasing masses of the stop and sbottom quarks from P1 to P4 (which makes the final state leptons, jets and missing energy more and more harder) the efficiencies of M_{T2} and m_{eff} increase for the signal events. These two steps also reduce the backgrounds to a manageable level. In the final step, the demand of a top quark in the sample brings down the background to a minuscule level keeping a handful of signal events.

In Table 4 we give a summary of our signal and background events and also estimate the signal significance (\mathcal{S}). While calculating the significance, in order to be conservative, we have also included a systematic uncertainty on the total background estimate. We thus define the significance \mathcal{S} to be,

$$\mathcal{S} = \frac{N_S}{\sqrt{N_B + (\kappa N_B)^2}}, \quad (2)$$

where N_S and N_B are the number of signal and background events respectively and κ is the measure of the systematic uncertainty. We will show our results for three choices of κ , 10%, 30% and 50%.

SM backgrounds	Production Cross-section (fb)	Simulated events (in units of 10^4)	No. of events after the cut					Final Cross-section (in units of 10^{-2} fb)
			C1	C2	C3	C4	C5	
$t\bar{t}$ + jets	918000 [111]	4320	1587596	601	39	29	4	8.5
tbW	61000	600	215807	80	4	2	1	1.0
$t\bar{t}Z$	1121 [112]	7	6255	253	52	20	2	3.2
$t\bar{t}W$	769 [113]	5	4471	31	3	2	1	1.5
$t\bar{t}W^+W^-$	10	1	1588	33	14	13	6	0.6
$t\bar{t}t\bar{t}$	10	1	1781	31	14	10	4	0.4
Total Background								15.2

Table 3: Event summary for the backgrounds after individual cuts as described in the text. In the last column we show the final cross-section after all the event selection cuts have been applied. For the $t\bar{t}$ + jets background we have generated a matched sample of $t\bar{t}$ + 0 jet, $t\bar{t}$ + 1 jet and $t\bar{t}$ + 2 jets using Madgraph.

		Signal(N_S) (Background(N_B))			Significance(\mathcal{S}) for $\kappa = 10\%$ (30%, 50%)		
	$m_{\bar{t}_1}$ (GeV)	10 fb^{-1}	50 fb^{-1}	100 fb^{-1}	10 fb^{-1}	50 fb^{-1}	100 fb^{-1}
P1	501.6	6.2(1.6)	31.1(8)	62.2(16)	4.9(4.6, 4.1)	10.8(8.4, 6.3)	14.4(9.9, 6.9)
P2	501.6	6.2(1.6)	31.1(8)	62.2(16)	4.9(4.6, 4.1)	10.8(8.4, 6.3)	14.4(9.9, 6.9)
P3	714.2	4.1(1.6)	20.7(8)	41.3(16)	3.2(3.0, 2.7)	7.0(5.6, 4.2)	9.6(6.6, 4.6)
P4	714.2	4.1(1.6)	20.7(8)	41.3(16)	3.2(3.0, 2.7)	7.0(5.6, 4.2)	9.6(6.6, 4.6)
P5	918.1	1.6(1.6)	7.9(8)	15.9(16)	1.3(1.2, 1.1)	2.7(2.1, 1.6)	3.7(2.5, 1.8)
P6	918.1	1.7(1.6)	8.7(8)	17.4(16)	1.3(1.2, 1.1)	2.9(2.3, 1.8)	4.0(2.8, 1.9)

Table 4: The summary of our signal and backgrounds. Columns 3-5 show the number of signal (total background) events for three values of the integrated luminosity: 10 fb^{-1} , 50 fb^{-1} and 100 fb^{-1} . The columns 6-8 show the statistical significance of our signal for the above three integrated luminosities. For each value of the integrated luminosity the significance is shown for three choices of the amount of possible systematic uncertainties, $\kappa = 10\%$, 30% and 50%.

Note that in principle, a detailed detector simulation has to be performed to check the robustness of our analysis. However, a true detector simulation is completely outside the scope of this work. In order to roughly estimate the detector effects on the efficiencies of the individual cuts in Table 2 we have made our Madgraph/Pythia generated events for some of the signal points pass through the public detector simulation package Delphes [114] using the default ATLAS and CMS detector simulation cards provided by them. For the benchmark point P5, for example, we observe that the percentage of events which survived after the cut-2, 3, 4 and 5 are 17%(16%), 93%(94%), 91.8%(88.5%) and 19%(21.8%) respectively using the ATLAS(CMS) detector card as compared to 20%, 82.5%, 93.5% and 22.3% calculated from Table 2. We get similar results also for the other benchmark points as well as the backgrounds. Hence, we expect that the detector effects will not change our results to a significant extent and the uncertainty in our results due to these effects are safely taken care of by including the systematic uncertainty as mentioned in the previous paragraph.

Before we move to our next section, we would like to briefly discuss on relevance of soft radiation and pileups effects on the jet substructure algorithm. It is well known that at higher collision energy and high luminosity run of the LHC, in the hadronic final states it will be very challenging to isolate high p_T events in the presence of the large number of additional soft pp collisions, pileup (PU) that occur simultaneously with

any hard interactions. These low p_T phenomena will adversely affect the absolute energy measurements of jets. Hence, it is of particular interest to understand the sensitivity of large size jets in presence of pileup. Grooming techniques may serve to mitigate pileup sensitivity by effectively reducing the jet area. Jet grooming methods (e.g., filtering [115], trimming [116], pruning [117]) were designed exactly for this purpose to remove the soft uncorrelated radiation from the fat jet while retaining the final state radiation off the resonance. Some recent analysis based on the leading order parton-shower Monte Carlo have been seen to agree with the data quite well [118, 119] after these grooming algorithms were used. Although it is impossible for us to simulate events including pileup and provide a quantitative estimate of its effect, we believe that the pileup contamination will not change our results in a significant way, in view of the efficient grooming techniques which seem to work pretty well even on the real data.

4 Interpretation in simplified scenarios

In this section we interpret our results in two simplified model scenarios. In the first model we consider direct stop pair production and their decay through the decay chain

$$pp \rightarrow \tilde{t}_1 \tilde{t}_1^*, \tilde{t}_1 \rightarrow t \tilde{\chi}_2^0, \tilde{\chi}_2^0 \rightarrow \tilde{\chi}_1^0 Z,$$

while in the second case we study the direct sbottom pair production using the following decay chain

$$pp \rightarrow \tilde{b}_1 \tilde{b}_1^*, \tilde{b}_1 \rightarrow t \tilde{\chi}_1^-, \tilde{\chi}_1^- \rightarrow \tilde{\chi}_1^0 W^-.$$

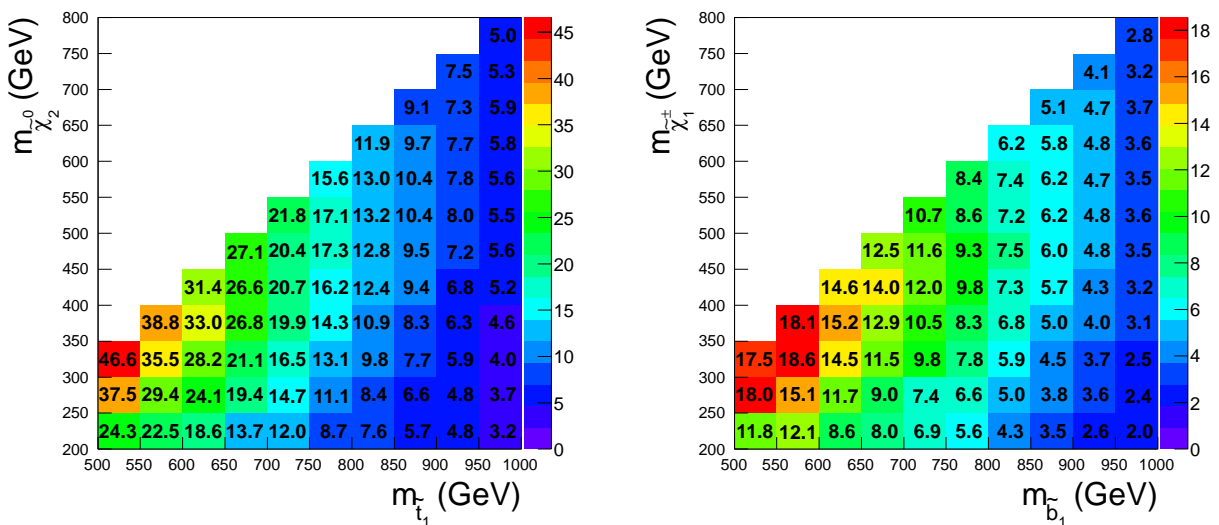


Figure 5: The signal significance at 100 fb^{-1} in the \tilde{t}_1 - $\tilde{\chi}_2^0$ plane (left panel) and \tilde{b}_1 - $\tilde{\chi}_1^\pm$ plane (right panel) in the two simplified model scenarios as described in the text.

We assume all the branching ratios to be unity. In Fig. 5 we show the estimate of our signal significance calculated in the same way as in the previous section (with $\kappa = 10\%$) corresponding to a 100 fb^{-1} data set. The figure in the left panel shows the significance in the \tilde{t}_1 - $\tilde{\chi}_2^0$ plane for our first simplified model while the figure in the right panel presents the significance in the \tilde{b}_1 - $\tilde{\chi}_1^\pm$ plane in the second model. In both cases we assume the mass of the lightest neutralino to be 50 GeV. It can be observed that a top squark mass of about 1 TeV can be probed with 4- 5σ significance in the first case and sbottoms of mass about 900 GeV can be discovered with the same significance in the latter case.

5 Summary and Conclusion

The non-observation of gluinos and squarks of first two generations and the discovery of a SM like higgs boson with mass around 125 GeV has forced us to consider the possibility of the existence of a light third generation of squarks namely, the top and the bottom quarks. As a light third generation of squarks is also motivated by naturalness arguments, searches of such light stop and sbottoms in all possible decay topologies are extremely important in the endeavour to look for signals of supersymmetry at the LHC. The production cross-section of a TeV scale stop or sbottom pairs being rather small, it is useful to consider an inclusive search strategy for stop and sbottom pair production in a common final state. In this work we attempt to perform such a study choosing a final state containing a top quark and two additional hard leptons along with substantial missing transverse momentum. We carry out a detailed simulation of the signal and all the possible backgrounds and observe that the combined use of di-leptonic M_{T2} , the effective mass of an event m_{eff} and the jet substructure technique to tag a hadronically decaying top is extremely useful to achieve a good signal significance. We find that a third generation of squarks with masses about 900 GeV can be discovered at the 14 TeV LHC with a 100 fb^{-1} data set which is achievable within the first few years of LHC14 run. We also interpret our results in the context of two simplified models of light stop and light sbottom squarks and conclude that with our strategy top squarks up to 1 TeV and bottom squarks up to about 900 GeV can be discovered with the same amount of data.

It is our hope that this work will motivate the experimental collaborations to perform further detailed analysis of the proposed channel on the real data taking our work as a starting guide.

6 Acknowledgements

DG acknowledges support from ERC Ideas Starting Grant n.279972 “NPFlavour”. DG thanks Satoshi Mishima for discussions and help in making some of the figures using ROOT. DG and DS also thank Monoranjan Guchait for encouragement and support and Sanmay Ganguly and Rajdeep M. Chatterjee of the CMS collaboration for discussion and help with some aspects of the software ROOT.

References

- [1] **ATLAS Collaboration** Collaboration, G. Aad et al., “The ATLAS Experiment at the CERN Large Hadron Collider,” *JINST* **3** (2008) S08003.
- [2] **CMS Collaboration** Collaboration, S. Chatrchyan et al., “The CMS experiment at the CERN LHC,” *JINST* **3** (2008) S08004.
- [3] **CMS Collaboration**, S. Chatrchyan et al., “Observation of a new boson at a mass of 125 GeV with the CMS experiment at the LHC,” *Phys.Lett.* **B716** (2012) 30–61, [arXiv:1207.7235 \[hep-ex\]](#).
- [4] **ATLAS Collaboration**, G. Aad et al., “Observation of a new particle in the search for the Standard Model Higgs boson with the ATLAS detector at the LHC,” *Phys.Lett.* **B716** (2012) 1–29, [arXiv:1207.7214 \[hep-ex\]](#).
- [5] H. Baer, V. Barger, and A. Mustafayev, “Implications of a 125 GeV Higgs scalar for LHC SUSY and neutralino dark matter searches,” *Phys.Rev.* **D85** (2012) 075010, [arXiv:1112.3017 \[hep-ph\]](#).
- [6] S. Akula, B. Altunkaynak, D. Feldman, P. Nath, and G. Peim, “Higgs Boson Mass Predictions in SUGRA Unification, Recent LHC-7 Results, and Dark Matter,” *Phys.Rev.* **D85** (2012) 075001, [arXiv:1112.3645 \[hep-ph\]](#).
- [7] J. L. Feng, K. T. Matchev, and D. Sanford, “Focus Point Supersymmetry Redux,” *Phys.Rev.* **D85** (2012) 075007, [arXiv:1112.3021 \[hep-ph\]](#).
- [8] S. Heinemeyer, O. Stal, and G. Weiglein, “Interpreting the LHC Higgs Search Results in the MSSM,” *Phys.Lett.* **B710** (2012) 201–206, [arXiv:1112.3026 \[hep-ph\]](#).

- [9] O. Buchmueller, R. Cavanaugh, A. De Roeck, M. Dolan, J. Ellis, et al., “Higgs and Supersymmetry,” *Eur.Phys.J.* **C72** (2012) 2020, [arXiv:1112.3564 \[hep-ph\]](#).
- [10] P. Draper, P. Meade, M. Reece, and D. Shih, “Implications of a 125 GeV Higgs for the MSSM and Low-Scale SUSY Breaking,” *Phys.Rev.* **D85** (2012) 095007, [arXiv:1112.3068 \[hep-ph\]](#).
- [11] J. Cao, Z. Heng, D. Li, and J. M. Yang, “Current experimental constraints on the lightest Higgs boson mass in the constrained MSSM,” *Phys.Lett.* **B710** (2012) 665–670, [arXiv:1112.4391 \[hep-ph\]](#).
- [12] L. J. Hall, D. Pinner, and J. T. Ruderman, “A Natural SUSY Higgs Near 126 GeV,” *JHEP* **1204** (2012) 131, [arXiv:1112.2703 \[hep-ph\]](#).
- [13] J. Ellis and K. A. Olive, “Revisiting the Higgs Mass and Dark Matter in the CMSSM,” *Eur.Phys.J.* **C72** (2012) 2005, [arXiv:1202.3262 \[hep-ph\]](#).
- [14] H. Baer, V. Barger, and A. Mustafayev, “Neutralino dark matter in mSUGRA/CMSSM with a 125 GeV light Higgs scalar,” *JHEP* **1205** (2012) 091, [arXiv:1202.4038 \[hep-ph\]](#).
- [15] L. Maiani, A. Polosa, and V. Riquer, “Probing Minimal Supersymmetry at the LHC with the Higgs Boson Masses,” *New J.Phys.* **14** (2012) 073029, [arXiv:1202.5998 \[hep-ph\]](#).
- [16] T. Cheng, J. Li, T. Li, D. V. Nanopoulos, and C. Tong, “Electroweak Supersymmetry around the Electroweak Scale,” [arXiv:1202.6088 \[hep-ph\]](#).
- [17] J.-J. Cao, Z.-X. Heng, J. M. Yang, Y.-M. Zhang, and J.-Y. Zhu, “A SM-like Higgs near 125 GeV in low energy SUSY: a comparative study for MSSM and NMSSM,” *JHEP* **1203** (2012) 086, [arXiv:1202.5821 \[hep-ph\]](#).
- [18] F. Brummer, S. Kraml, and S. Kulkarni, “Anatomy of maximal stop mixing in the MSSM,” *JHEP* **1208** (2012) 089, [arXiv:1204.5977 \[hep-ph\]](#).
- [19] C. Balazs, A. Buckley, D. Carter, B. Farmer, and M. White, “Should we still believe in constrained supersymmetry?,” [arXiv:1205.1568 \[hep-ph\]](#).
- [20] J. L. Feng and D. Sanford, “A Natural 125 GeV Higgs Boson in the MSSM from Focus Point Supersymmetry with A-Terms,” *Phys.Rev.* **D86** (2012) 055015, [arXiv:1205.2372 \[hep-ph\]](#).
- [21] D. Ghosh, M. Guchait, S. Raychaudhuri, and D. Sengupta, “How Constrained is the cMSSM?,” *Phys.Rev.* **D86** (2012) 055007, [arXiv:1205.2283 \[hep-ph\]](#).
- [22] A. Fowlie, M. Kazana, K. Kowalska, S. Munir, L. Roszkowski, et al., “The CMSSM Favoring New Territories: The Impact of New LHC Limits and a 125 GeV Higgs,” *Phys.Rev.* **D86** (2012) 075010, [arXiv:1206.0264 \[hep-ph\]](#).
- [23] P. Athron, S. King, D. Miller, S. Moretti, and R. Nevzorov, “Constrained Exceptional Supersymmetric Standard Model with a Higgs Near 125 GeV,” *Phys.Rev.* **D86** (2012) 095003, [arXiv:1206.5028 \[hep-ph\]](#).
- [24] M. W. Cahill-Rowley, J. L. Hewett, A. Ismail, and T. G. Rizzo, “The Higgs Sector and Fine-Tuning in the pMSSM,” *Phys.Rev.* **D86** (2012) 075015, [arXiv:1206.5800 \[hep-ph\]](#).
- [25] S. Akula, P. Nath, and G. Peim, “Implications of the Higgs Boson Discovery for mSUGRA,” *Phys.Lett.* **B717** (2012) 188–192, [arXiv:1207.1839 \[hep-ph\]](#).
- [26] J. Cao, Z. Heng, J. M. Yang, and J. Zhu, “Status of low energy SUSY models confronted with the LHC 125 GeV Higgs data,” *JHEP* **1210** (2012) 079, [arXiv:1207.3698 \[hep-ph\]](#).
- [27] A. Arbey, M. Battaglia, A. Djouadi, and F. Mahmoudi, “The Higgs sector of the phenomenological MSSM in the light of the Higgs boson discovery,” *JHEP* **1209** (2012) 107, [arXiv:1207.1348 \[hep-ph\]](#).

- [28] P. Nath, “SUGRA Grand Unification, LHC and Dark Matter,” [arXiv:1207.5501 \[hep-ph\]](#).
- [29] J. Ellis, F. Luo, K. A. Olive, and P. Sandick, “The Higgs Mass beyond the CMSSM,” [arXiv:1212.4476 \[hep-ph\]](#).
- [30] M. Chakraborti, U. Chattopadhyay, and R. M. Godbole, “Implication of Higgs at 125 GeV within Stochastic Superspace Framework,” [arXiv:1211.1549 \[hep-ph\]](#).
- [31] A. Chakraborty, B. Das, J. L. Diaz-Cruz, D. K. Ghosh, S. Moretti, et al., “The 125 GeV Higgs signal at the LHC in the CP Violating MSSM,” [arXiv:1301.2745 \[hep-ph\]](#).
- [32] V. E. Mayes, “SUSY into Darkness: Heavy Scalars in the CMSSM,” [arXiv:1302.4394 \[hep-ph\]](#).
- [33] A. Dighe, D. Ghosh, K. M. Patel, and S. Raychaudhuri, “Testing Times for Supersymmetry: Looking Under the Lamp Post,” [arXiv:1303.0721 \[hep-ph\]](#).
- [34] D. Ghosh, M. Guchait, and D. Sengupta, “Higgs Signal in Chargino-Neutralino Production at the LHC,” *Eur.Phys.J. C* **72** (2012) 2141, [arXiv:1202.4937 \[hep-ph\]](#).
- [35] A. Choudhury and A. Datta, “Many faces of low mass neutralino dark matter in the unconstrained MSSM, LHC data and new signals,” *JHEP* **1206** (2012) 006, [arXiv:1203.4106 \[hep-ph\]](#).
- [36] P. Byakti and D. Ghosh, “Magic Messengers in Gauge Mediation and signal for 125 GeV boosted Higgs boson,” *Phys.Rev.* **D86** (2012) 095027, [arXiv:1204.0415 \[hep-ph\]](#).
- [37] R. M. Chatterjee, M. Guchait, and D. Sengupta, “Probing Supersymmetry using Event Shape variables at 8 TeV LHC,” *Phys.Rev.* **D86** (2012) 075014, [arXiv:1206.5770 \[hep-ph\]](#).
- [38] H. Baer, V. Barger, A. Lessa, and X. Tata, “Discovery potential for SUSY at a high luminosity upgrade of LHC14,” *Phys.Rev.* **D86** (2012) 117701, [arXiv:1207.4846 \[hep-ph\]](#).
- [39] K. Howe and P. Saraswat, “Excess Higgs Production in Neutralino Decays,” *JHEP* **1210** (2012) 065, [arXiv:1208.1542 \[hep-ph\]](#).
- [40] D. Ghosh and D. Sengupta, “Searching the sbottom in the four lepton channel at the LHC,” [arXiv:1209.4310 \[hep-ph\]](#).
- [41] D. Ghosh, R. Godbole, M. Guchait, K. Mohan, and D. Sengupta, “Looking for an Invisible Higgs Signal at the LHC,” [arXiv:1211.7015 \[hep-ph\]](#).
- [42] A. Arbey, M. Battaglia, and F. Mahmoudi, “Higgs Production in Neutralino Decays in the MSSM - The LHC and a Future e+e- Collider,” [arXiv:1212.6865 \[hep-ph\]](#).
- [43] B. Bhattacharjee, A. Chakraborty, D. Kumar Ghosh, and S. Raychaudhuri, “Using Jet Substructure at the LHC to Search for the Light Higgs Bosons of the CP-Violating MSSM,” *Phys.Rev.* **D86** (2012) 075012, [arXiv:1204.3369 \[hep-ph\]](#).
- [44] D. Ghosh, “Boosted di-boson from a mixed heavy stop,” [arXiv:1308.0320 \[hep-ph\]](#).
- [45] G. Belanger, D. Ghosh, R. Godbole, M. Guchait, and D. Sengupta, “Probing the flavor violating scalar top quark signal at the LHC,” [arXiv:1308.6484 \[hep-ph\]](#).
- [46] J. Berger, J. Hubisz, and M. Perelstein, “A Fermionic Top Partner: Naturalness and the LHC,” *JHEP* **1207** (2012) 016, [arXiv:1205.0013 \[hep-ph\]](#).
- [47] J. Cao, C. Han, L. Wu, J. M. Yang, and Y. Zhang, “Probing Natural SUSY from Stop Pair Production at the LHC,” [arXiv:1206.3865 \[hep-ph\]](#).
- [48] L. Randall and M. Reece, “Single-Scale Natural SUSY,” [arXiv:1206.6540 \[hep-ph\]](#).
- [49] J. R. Espinosa, C. Grojean, V. Sanz, and M. Trott, “NSUSY fits,” *JHEP* **1212** (2012) 077, [arXiv:1207.7355 \[hep-ph\]](#).

- [50] “Search for supersymmetry with the razor variables at CMS,” Tech. Rep. CMS PAS SUS-12-005, CERN, Geneva, 2012.
- [51] “Search for squarks and gluinos with the ATLAS detector using final states with jets and missing transverse momentum and 5.8 fb^{-1} of $\sqrt{s}=8$ TeV proton-proton collision data,” Tech. Rep. ATLAS-CONF-2012-109, CERN, Geneva, Aug, 2012.
- [52] “Search for supersymmetry in events with large missing transverse momentum, jets, and at least one tau lepton in 21 fb^{-1} of $\sqrt{s} = 8$ tev proton-proton collision data with the atlas detector,” Tech. Rep. ATLAS-CONF-2013-026, CERN, Geneva, Mar, 2013.
- [53] “Search for supersymmetry in events with four or more leptons in 21 fb^{-1} of pp collisions at $\sqrt{s} = 8$ tev with the atlas detector,” Tech. Rep. ATLAS-CONF-2013-036, CERN, Geneva, Mar, 2013.
- [54] “Search for rpv susy in the four-lepton final state,” Tech. Rep. CMS-PAS-SUS-13-010, CERN, Geneva, 2013.
- [55] “Search for light stop rpv supersymmetry with three or more leptons and b-tags,” Tech. Rep. CMS-PAS-SUS-13-003, CERN, Geneva, 2013.
- [56] N. Desai and B. Mukhopadhyaya, “Constraints on supersymmetry with light third family from LHC data,” *JHEP* **1205** (2012) 057, [arXiv:1111.2830 \[hep-ph\]](#).
- [57] B. He, T. Li, and Q. Shafi, “Impact of LHC Searches on NLSP Top Squark and Gluino Mass,” *JHEP* **1205** (2012) 148, [arXiv:1112.4461 \[hep-ph\]](#).
- [58] M. Drees, M. Hanussek, and J. S. Kim, “Light Stop Searches at the LHC with Monojet Events,” *Phys.Rev.* **D86** (2012) 035024, [arXiv:1201.5714 \[hep-ph\]](#).
- [59] T. Plehn, M. Spannowsky, and M. Takeuchi, “Stop searches in 2012,” *JHEP* **1208** (2012) 091, [arXiv:1205.2696 \[hep-ph\]](#).
- [60] Z. Han, A. Katz, D. Krohn, and M. Reece, “(Light) Stop Signs,” *JHEP* **1208** (2012) 083, [arXiv:1205.5808 \[hep-ph\]](#).
- [61] V. Barger, P. Huang, M. Ishida, and W.-Y. Keung, “Scalar-Top Masses from SUSY Loops with 125 GeV mh and Precise Mw,” [arXiv:1206.1777 \[hep-ph\]](#).
- [62] A. Choudhury and A. Datta, “New limits on top squark NLSP from LHC 4.7 fb^{-1} data,” *Mod.Phys.Lett.* **A27** (2012) 1250188, [arXiv:1207.1846 \[hep-ph\]](#).
- [63] C.-Y. Chen, A. Freitas, T. Han, and K. S. Lee, “New Physics from the Top at the LHC,” [arXiv:1207.4794 \[hep-ph\]](#).
- [64] S. Bornhauser, M. Drees, S. Grab, and J. Kim, “Light Stop Searches at the LHC in Events with two b-Jets and Missing Energy,” *Phys.Rev.* **D83** (2011) 035008, [arXiv:1011.5508 \[hep-ph\]](#).
- [65] S. Kraml and A. Raklev, “Same-sign top quarks as signature of light stops at the LHC,” *Phys.Rev.* **D73** (2006) 075002, [arXiv:hep-ph/0512284 \[hep-ph\]](#).
- [66] Z.-H. Yu, X.-J. Bi, Q.-S. Yan, and P.-F. Yin, “Detecting light stop pairs in coannihilation scenarios at the LHC,” [arXiv:1211.2997 \[hep-ph\]](#).
- [67] M. A. Ajaib, T. Li, and Q. Shafi, “Stop-Neutralino Coannihilation in the Light of LHC,” *Phys.Rev.* **D85** (2012) 055021, [arXiv:1111.4467 \[hep-ph\]](#).
- [68] K. Ghosh, K. Huitu, J. Laamanen, L. Leinonen, K. Huitu, et al., “Top jets as a probe of degenerate stop-NLSP LSP scenario in the framework of cMSSM,” [arXiv:1207.2429 \[hep-ph\]](#).
- [69] B. Dutta, T. Kamon, N. Kolev, K. Sinha, and K. Wang, “Searching for Top Squarks at the LHC in Fully Hadronic Final State,” *Phys.Rev.* **D86** (2012) 075004, [arXiv:1207.1873 \[hep-ph\]](#).

- [70] D. S. Alves, M. R. Buckley, P. J. Fox, J. D. Lykken, and C.-T. Yu, “Stops and MET: The Shape of Things to Come,” [arXiv:1205.5805 \[hep-ph\]](#).
- [71] D. Berenstein, T. Liu, and E. Perkins, “Multiple b-jets reveal natural SUSY and the 125 GeV Higgs,” [arXiv:1211.4288 \[hep-ph\]](#).
- [72] C. Kilic and B. Tweedie, “Cornering Light Stops with Dileptonic mT_2 ,” [arXiv:1211.6106 \[hep-ph\]](#).
- [73] M. Adeel Ajaib, T. Li, and Q. Shafi, “Searching for NLSP Sbottom at the LHC,” *Phys.Lett.* **B701** (2011) 255–259, [arXiv:1104.0251 \[hep-ph\]](#).
- [74] H. M. Lee, V. Sanz, and M. Trott, “Hitting sbottom in natural SUSY,” *JHEP* **1205** (2012) 139, [arXiv:1204.0802 \[hep-ph\]](#).
- [75] E. Alvarez and Y. Bai, “Reach the Bottom Line of the Sbottom Search,” *JHEP* **1208** (2012) 003, [arXiv:1204.5182 \[hep-ph\]](#).
- [76] M. A. Ajaib, I. Gogoladze, and Q. Shafi, “Higgs Boson Production and Decay: Effects from Light Third Generation and Vectorlike Matter,” [arXiv:1207.7068 \[hep-ph\]](#).
- [77] T. Plehn, M. Spannowsky, M. Takeuchi, and D. Zerwas, “Stop Reconstruction with Tagged Tops,” *JHEP* **1010** (2010) 078, [arXiv:1006.2833 \[hep-ph\]](#).
- [78] D. E. Kaplan, K. Rehermann, and D. Stolarski, “Searching for Direct Stop Production in Hadronic Top Data at the LHC,” *JHEP* **1207** (2012) 119, [arXiv:1205.5816 \[hep-ph\]](#).
- [79] J. Berger, M. Perelstein, M. Saelim, and A. Spray, “Boosted Tops from Gluino Decays,” [arXiv:1111.6594 \[hep-ph\]](#).
- [80] P. Bandyopadhyay and B. Bhattacharjee, “Boosted top quarks in supersymmetric cascade decays at the LHC,” *Phys.Rev.* **D84** (2011) 035020, [arXiv:1012.5289 \[hep-ph\]](#).
- [81] **CMS Collaboration** Collaboration, S. Chatrchyan et al., “Search for new physics in events with same-sign dileptons and b jets in pp collisions at $\sqrt{s} = 8$ TeV,” [arXiv:1212.6194 \[hep-ex\]](#).
- [82] “Search for direct stop production in events with missing transverse momentum and two b-jets using 12.8 fb^{-1} of pp collisions at $\sqrt{s} = 8$ tev with the atlas detector,” Tech. Rep. ATLAS-CONF-2013-001, CERN, Geneva, Jan, 2013.
- [83] “Search for direct top squark pair production in final states with one isolated lepton, jets, and missing transverse momentum in $\sqrt{s} = 8, \text{tev}$ pp collisions using 21 fb^{-1} of atlas data,” Tech. Rep. ATLAS-CONF-2013-037, CERN, Geneva, Mar, 2013.
- [84] “Search for direct third generation squark pair production in final states with missing transverse momentum and two b -jets in $\sqrt{s} = 8$ tev pp collisions with the atlas detector.,” Tech. Rep. ATLAS-CONF-2013-053, CERN, Geneva, May, 2013.
- [85] “Search for direct top squark pair production in final states with two leptons in $\sqrt{s} = 8$ tev pp collisions using 20 fb^{-1} of atlas data.,” Tech. Rep. ATLAS-CONF-2013-048, CERN, Geneva, May, 2013.
- [86] “Search for direct stop pair production in events with a z boson, b-jets and missing transverse energy with the atlas detector using 21 fb^{-1} from proton-proton collision at $\sqrt{s} = 8$ tev,” Tech. Rep. ATLAS-CONF-2013-025, CERN, Geneva, Mar, 2013.
- [87] **ATLAS Collaboration** Collaboration, G. Aad et al., “Search for light top squark pair production in final states with leptons and b^- jets with the ATLAS detector in $\sqrt{s} = 7$ TeV proton-proton collisions,” *Phys.Lett.* **B720** (2013) 13–31, [arXiv:1209.2102 \[hep-ex\]](#).

- [88] **ATLAS Collaboration** Collaboration, G. Aad et al., “Search for light scalar top quark pair production in final states with two leptons with the ATLAS detector in $\sqrt{s} = 7$ TeV proton-proton collisions,” *Eur.Phys.J.* **C72** (2012) 2237, [arXiv:1208.4305 \[hep-ex\]](#).
- [89] **ATLAS Collaboration** Collaboration, G. Aad et al., “Search for a heavy top-quark partner in final states with two leptons with the ATLAS detector at the LHC,” *JHEP* **1211** (2012) 094, [arXiv:1209.4186 \[hep-ex\]](#).
- [90] “Search for top-squark pair production in the single lepton final state in pp collisions at 8 tev,” Tech. Rep. CMS-PAS-SUS-13-011, CERN, Geneva, 2013.
- [91] “Search for supersymmetry in pp collisions at $\sqrt{s} = 8$ tev in events with three leptons and at least one b-tagged jet,” Tech. Rep. CMS-PAS-SUS-13-008, CERN, Geneva, 2013.
- [92] M. L. Graesser and J. Shelton, “Hunting Asymmetric Stops,” [arXiv:1212.4495 \[hep-ph\]](#).
- [93] B. Dutta, T. Kamon, N. Koley, K. Sinha, K. Wang, et al., “Top Squark Searches Using Dilepton Invariant Mass Distributions and Bino-Higgsino Dark Matter at the LHC,” [arXiv:1302.3231 \[hep-ph\]](#).
- [94] “Search for direct production of charginos and neutralinos in events with three leptons and missing transverse momentum in 13.0 fb⁻¹ of pp collisions at $\sqrt{s}=8$ tev with the atlas detector,” Tech. Rep. ATLAS-CONF-2012-154, CERN, Geneva, Nov, 2012.
- [95] “Search for direct ewk production of susy particles in multilepton modes with 8tev data,” Tech. Rep. CMS-PAS-SUS-12-022, CERN, Geneva, 2013.
- [96] “Search for direct production of charginos and neutralinos in events with three leptons and missing transverse momentum in 21 fb⁻¹ of pp collisions at $\sqrt{s} = 8$ tev with the atlas detector,” Tech. Rep. ATLAS-CONF-2013-035, CERN, Geneva, Mar, 2013.
- [97] A. Djouadi, J.-L. Kneur, and G. Moultaka, “SuSpect: A Fortran code for the supersymmetric and Higgs particle spectrum in the MSSM,” *Comput.Phys.Commun.* **176** (2007) 426–455, [arXiv:hep-ph/0211331 \[hep-ph\]](#).
- [98] A. Djouadi, M. Muhlleitner, and M. Spira, “Decays of supersymmetric particles: The Program SUSY-HIT (SUSpect-SdecaY-Hdecay-InTerface),” *Acta Phys.Polon.* **B38** (2007) 635–644, [arXiv:hep-ph/0609292 \[hep-ph\]](#).
- [99] W. Beenakker, R. Hopker, and M. Spira, “PROSPINO: A Program for the production of supersymmetric particles in next-to-leading order QCD,” [arXiv:hep-ph/9611232 \[hep-ph\]](#).
- [100] J. M. Campbell and F. Tramontano, “Next-to-leading order corrections to Wt production and decay,” *Nucl.Phys.* **B726** (2005) 109–130, [arXiv:hep-ph/0506289 \[hep-ph\]](#).
- [101] J. Campbell, R. K. Ellis, and R. Rntsch, “Single top production in association with a Z boson at the LHC,” [arXiv:1302.3856 \[hep-ph\]](#).
- [102] C. Lester and D. Summers, “Measuring masses of semiinvisibly decaying particles pair produced at hadron colliders,” *Phys.Lett.* **B463** (1999) 99–103, [arXiv:hep-ph/9906349 \[hep-ph\]](#).
- [103] A. Barr, C. Lester, and P. Stephens, “ $m(T_2)$: The Truth behind the glamour,” *J.Phys.* **G29** (2003) 2343–2363, [arXiv:hep-ph/0304226 \[hep-ph\]](#).
- [104] A. J. Barr and C. Gwenlan, “The Race for supersymmetry: Using $m(T_2)$ for discovery,” *Phys.Rev.* **D80** (2009) 074007, [arXiv:0907.2713 \[hep-ph\]](#).
- [105] D. E. Kaplan, K. Rehermann, M. D. Schwartz, and B. Tweedie, “Top Tagging: A Method for Identifying Boosted Hadronically Decaying Top Quarks,” *Phys.Rev.Lett.* **101** (2008) 142001, [arXiv:0806.0848 \[hep-ph\]](#).

- [106] Y. L. Dokshitzer, G. Leder, S. Moretti, and B. Webber, “Better jet clustering algorithms,” *JHEP* **9708** (1997) 001, [arXiv:hep-ph/9707323 \[hep-ph\]](#).
- [107] T. Sjostrand, S. Mrenna, and P. Z. Skands, “PYTHIA 6.4 Physics and Manual,” *JHEP* **0605** (2006) 026, [arXiv:hep-ph/0603175 \[hep-ph\]](#).
- [108] J. Alwall, M. Herquet, F. Maltoni, O. Mattelaer, and T. Stelzer, “MadGraph 5 : Going Beyond,” *JHEP* **1106** (2011) 128, [arXiv:1106.0522 \[hep-ph\]](#).
- [109] S. Hoeche, F. Krauss, N. Lavesson, L. Lonnblad, M. Mangano, et al., “Matching parton showers and matrix elements,” [arXiv:hep-ph/0602031 \[hep-ph\]](#).
- [110] M. Cacciari, G. P. Salam, and G. Soyez, “FastJet User Manual,” *Eur.Phys.J.* **C72** (2012) 1896, [arXiv:1111.6097 \[hep-ph\]](#).
- [111] N. Kidonakis, “Top Quark Theoretical Cross Sections and pT and Rapidity Distributions,” [arXiv:1109.3231 \[hep-ph\]](#).
- [112] A. Kardos, Z. Trocsanyi, and C. Papadopoulos, “Top quark pair production in association with a Z-boson at NLO accuracy,” *Phys.Rev.* **D85** (2012) 054015, [arXiv:1111.0610 \[hep-ph\]](#).
- [113] J. M. Campbell and R. K. Ellis, “ $t\bar{t}W^\pm$ production and decay at NLO,” *JHEP* **1207** (2012) 052, [arXiv:1204.5678 \[hep-ph\]](#).
- [114] S. Ovin, X. Rouby, and V. Lemaitre, “DELPHES, a framework for fast simulation of a generic collider experiment,” [arXiv:0903.2225 \[hep-ph\]](#).
- [115] J. M. Butterworth, A. R. Davison, M. Rubin, and G. P. Salam, “Jet substructure as a new Higgs search channel at the LHC,” *Phys.Rev.Lett.* **100** (2008) 242001, [arXiv:0802.2470 \[hep-ph\]](#).
- [116] D. Krohn, J. Thaler, and L.-T. Wang, “Jet Trimming,” *JHEP* **1002** (2010) 084, [arXiv:0912.1342 \[hep-ph\]](#).
- [117] S. D. Ellis, C. K. Vermilion, and J. R. Walsh, “Techniques for improved heavy particle searches with jet substructure,” *Phys.Rev.* **D80** (2009) 051501, [arXiv:0903.5081 \[hep-ph\]](#).
- [118] **CMS Collaboration** Collaboration, S. Chatrchyan et al., “Studies of jet mass in dijet and W/Z + jet events,” *JHEP* **1305** (2013) 090, [arXiv:1303.4811 \[hep-ex\]](#).
- [119] **ATLAS Collaboration** Collaboration, G. Aad et al., “Performance of jet substructure techniques for large-R jets in proton-proton collisions at $\sqrt{s} = 7$ TeV using the ATLAS detector,” [arXiv:1306.4945 \[hep-ex\]](#).